



Continuous methane concentration measurements at the Greenland Ice Sheet-atmosphere interface using a low-cost low-power metal oxide sensor system

5 Christian Juncher Jørgensen¹, Jacob Mønster², Karsten Fuglsang², Jesper Riis Christiansen³

¹Department of Bioscience, Arctic Environment, Aarhus University, Roskilde, 4000, Denmark

²FORCE Technology, Brøndby, 2605, Denmark

³Department of Geoscience and Natural Resources, University of Copenhagen, Frederiksberg C, 1958, Denmark

10 *Correspondence to:* Christian Juncher Jørgensen (cjj@bios.au.dk)

Abstract. In this paper, the performance of a low-cost and low-power methane (CH₄) sensing system prototype based on a metal oxide sensor (MOS) sensitive to CH₄ is tested in a natural CH₄ emitting environment at the Greenland Ice sheet (GrIS). We investigate if the MOS could be used as a supplementary measurement technique for monitoring CH₄ emissions from the GrIS with the scope of setting up a CH₄ monitoring network along the GrIS. The performance of the MOS is evaluated on
15 basis of parallel measurements using a CRDS reference instrument for CH₄ over a field calibration period of approximately 100 h. Results from the field calibration period show that CH₄ concentrations measured with the MOS is in very good agreement with the reference CRDS. The absolute concentration difference between the MOS and the CRDS reference values within the measured concentration range of approximately 2-100 ppm CH₄ were generally lower than 5 ppm CH₄, while the relative concentration deviations between the MOS and the CRDS were generally below 10 %. Calculated mean bias error for
20 the entire field calibration period was -0.05 ppm with a standard deviation of ± 1.69 ppm (n = 37,140). The results confirms that low-cost and low-power MOS can be effectively used for atmospheric CH₄ measurements under stable water vapor conditions. The primary scientific importance of the study is that it provides a clear example on how the application of low cost technology can enhance our future understanding on the climatic feedbacks from the cryosphere to the atmosphere.

1. Introduction

25 Constraining the various sources and sinks in the global methane (CH₄) budget is becoming an increasingly important parameter in mitigating climate change (Saunois et al., 2016). While the Arctic is generally considered a major global emitter of CH₄ to the atmosphere, significant uncertainty exists to the seasonal dynamics and strength of both CH₄ sources and CH₄ sinks from both terrestrial and marine environments, as well as the cryosphere (Callaghan et al., 2011; Emmerton et al., 2014; Juncher Jørgensen et al., 2015; Pirk et al., 2017; Zona et al., 2016). Recently, a previously unknown source of CH₄ emission
30 to the atmosphere was identified where CH₄ is emitted from meltwater originating in the subglacial domain of the Greenland Ice Sheet (GrIS) (Christiansen and Jørgensen, 2018; Lamarche-Gagnon et al., 2018; Wadham et al., 2019). The spatiotemporal



35 coverage of the new CH₄ source is yet to be determined and the overall climatic importance of this new component in the Arctic CH₄ budget is still unknown. Future studies are needed in order to assess the overall climatic significance of this source of CH₄ emission from the cryosphere to the atmosphere. The current state of knowledge on the CH₄ exchange from Greenland is inherently limited by the remoteness of many field sites with following high expedition cost and limitations to the spatial coverage and temporal duration of field measurements. Adding to this is the financial and logistical challenges of bringing high precision analyzers into the field, keeping them powered, running and shielded in the harsh environments often encountered in the Arctic. Thus, there is substantial potential and need to develop low-power techniques and measurement systems that can perform reliable autonomous CH₄ concentration measurements. The emergence of low-cost/low-power sensor technology in recent years provides an opportunity to overcome many of current restraints on obtaining continuous field measurements from a wide range of natural CH₄ emitting systems (wetlands, ice sheets, marine gas seeps, lakes, permafrost) and expand the network of continuous measurements in remote areas maximizing our understanding of these systems and minimizing the risk of losing valuable analytical equipment.

45 Low-cost metal oxide gas sensors (MOS) have been widely used for sensing various gases under atmospheric conditions (Wang et al., 2010). However, MOS sensors have significant obstacles to their direct use as air quality monitors as their output signal is influenced by the concentrations of both the target and interfering gases, as well as the temperature and humidity effects (Masson et al., 2015; Sohn et al., 2008). Other known challenges to the use of MOS are baseline drift over time, caused by either changes in the heat output of the sensing element or due to poisoning of the sensor surface (Peterson et al., 2017).

50 In recent years, investigations into the performance of CH₄ sensitive MOS sensors for the measurement of atmospheric CH₄ have been made under both natural and controlled conditions (van den Bossche et al., 2017; Eugster and Kling, 2012; Penza et al., 2015). These studies have been prompted by an increased interest in finding effective methods to quantify CH₄ emissions to the atmosphere from both natural systems and man-made systems such as landfills or biogas production plants. Using sensor specific post-processing to compensate for variations in relative humidity and air temperature, the previous studies have demonstrated a high potential for the low-cost and low-power monitoring of CH₄ concentrations above the atmospheric background level for various applications and in sensor network grids. In the current study, we have in situ tested the performance of a CH₄ sensitive MOS (Figaro TGS2611-E00) against a state-of-the-art cavity ring-down spectrometer for CH₄ (Ultra-portable Greenhouse Gas Analyzer, Los Gatos Research Inc.) to measure CH₄ concentrations in the air expelled from a subglacial meltwater outlet at GrIS. This was done to assess the MOS's potential for serving as a sensing element in future studies of the important scientific knowledge gap concerning the climatic feedbacks following CH₄ emissions from the subglacial domain under the Greenland Ice Sheet to the atmosphere.



2. Materials and methods

65

2.1 Field site and instrumentation

The study site is located on the southern flank at the terminus of the Isunnguata Sermia Glacier at the western margin of the GrIS (67°09'16.40''N 50°04'08.48''W) at an elevation of 450 meter above sea level (Fig. 1). At a small subglacial meltwater discharge outlet in this area, we performed measurements of CH₄ concentrations in the subglacial air expelled from naturally occurring caves carved out by meltwater below the ice sheet. The measurements were done in the period between June 22nd and 26th 2018. A more detailed description of the study site at the GrIS is given in (Christiansen and Jørgensen, 2018).

To sample the subglacial air the sampling tube was attached to an aluminum pole inserted approximately 5 meters into an ice cave with the inlet of the sampling tube connected to a 100 ml water trap (Fig. 2a). At the end of aluminum pole inside the subglacial cave the humidity and temperature of the subglacial air was measured every 10 seconds with a combined sensor (S-THB-M008, Onset, USA) connected to a datalogger (U30, Onset, USA). A sampling tube of 50 meter (inner diameter of 4 mm and total volume of 630 mL) was connected to the inlet of the CRDS (Ultraportable Greenhouse Gas Analyzer, Los Gatos Research, USA) for real-time reference concentration analysis of CH₄, carbon dioxide (CO₂) and water vapor (H₂O) (Fig. 2a). The diaphragm pump of the CRDS creates a constant flow of 800 mL min⁻¹. Through a 1 meter tube the outlet flow (800 mL min⁻¹) of the CRDS constantly flushed an open-ended enclosure (400 mL) in which the prototype CH₄ sensing system (MOS) was inserted (Fig. 2b). During the field calibration period (22nd to 26th July 2018), the rapid flushing of the air volume in the enclosure with the MOS system (2 times per minute) and the non-destructive sampling principle of the CRDS collectively ensured that the concentration of CH₄ in the above the MOS sensor was identical to the CRDS at the same time step.

Following the field calibration test of approximately 100 h, the MOS system was left as an autonomous monitoring system where a constant air-flow of approximately 3 L min⁻¹ to the enclosure with the MOS system was supplied by a 12 volt diaphragm pump (Thomas pumps, 1410VD DC) instead of using the outlet from the CRDS. During this period the system was powered by 12V LiFePO₄ batteries connected to solar panels and a voltage regulator. During the autonomous measuring period the MOS system and enclosure was placed in a water-proof case and buried under a pile of rocks to minimize the impact of sunlight induced temperature variations of the sensor system allowing a direct comparison between CH₄ concentration measurements of the CRDS and MOS systems.



2.2 The MOS system

The MOS system (Fig. 2c) consists of a microcontroller (Arduino Uno) and datalogger shield (DeekRobot data logging shield
95 V1.0) holding the board-mounted metal oxide CH₄ sensor (Figaro TGS 2611-E00) and an additional temperature/relative
humidity micro sensor (GY-21 HTU21). Logging frequency of the CRDS and MOS was 1 and 10 seconds, respectively. The
CH₄ sensitive MOS consists of a tin(IV)oxide (SnO₂) semiconductor which has low conductivity in clean air. In the presence
of CH₄, the sensor's conductivity increases depending on the gas concentration in the air (Kumar et al., 2009). A simple
electrical circuit convert the changes in conductivity at the sensing element as the gas concentrations vary to a change in output
100 voltage across the voltage divider (see Fig. 3). Both the heater and the sensing circuit of the MOS was powered by the 5 volt
regulated output of the Arduino Uno. The analogue output of the MOS was connected to the 10-bit analogue input on the
Arduino Uno using a 10 kOhm precision load-resistor in the voltage divider.

2.3 Laboratory calibration of the MOS sensor

105 In preparing for the field test of the CH₄ sensing system prototype, the MOS was performance tested and calibrated in a
controlled laboratory environment to evaluate both the response time to variations in methane concentration in the
concentration range 0-100 ppm CH₄ at three different levels of relative humidity (37±2 %, 55±3 % and 76±3 %). Synthetic air
(80 % N₂ and 20 % O₂) was used as zero gas for the laboratory test to which various concentrations of a CH₄ containing span
gas was mixed in using a HovaCAL calibration gas generator (IAS GmbH, Germany). After mixing of the zero gas and span
110 gas, the calibration gas was humidified using a water filled impinger similar to (van den Bossche et al., 2017). At each humidity
level, the output voltage from the MOS was logged using a Campbell CR1000 datalogger at a 2 second sampling frequency.
A pre-programmed calibration step sequence was used for all three humidity levels, consisting of time steps of each 10 minutes
in which the sensor was exposed to either zero gas or a calibration gas mixture in the applied the concentration range in an
alternating step pattern (Fig. 4). The temperature in the laboratory, zero gas, mixed calibration gas and water in impinger was
115 kept constant around 22 °C throughout the calibration test.

The sensor resistance (R_0) at exposure to the CH₄ free reference gas can be calculated at each of the three different humidity
levels according to Eq. (1):

$$120 \quad R_0 = \frac{V_C * R_L}{V_{OUT}} - R_L, \quad (1)$$

where V_C is the circuit voltage (i.e. 5 volt DC), R_L is the load resistance (10 kOhm) and V_{OUT} is the measured output voltage
(see also Eugster and Kling (2012) for further description).



125 The sensor resistance at various calibration gas concentrations (R_s) at different concentration steps in the calibration sequence can also be calculated using equation 1 for each of the three humidity levels (i.e. R_s replaces R_o in equation 1). For the tested type of MOS, the sensor resistance ratio (R_s/R_o) between the sensor resistance at a given concentration level (R_s) and the sensor resistance at the reference level (R_o) is inversely proportional to the absolute CH_4 concentration and can be modelled using e.g. a power fit (Fig. 5).

130 2.4 Field-calibration of the MOS

Field calibration of the MOS was done at the meltwater outlet at the Greenland Ice Sheet by parallel measurements of the same air mass by the MOS sensor system and a state-of-the-art CRDS. Since access to a controlled, humidified zero gas was not possible in the field, the output of the MOS when exposed to ambient air at the atmospheric background concentration of CH_4 (approximately 1.9 ppm) close to the ice sheet was used to calculate the average ambient sensor resistance (R_{0*}) using Eq. 1, which was then used to establish the resistance ratio (R_s/R_{0*}) vs. CH_4 concentration field calibration function for the MOS (Fig. 6).

2.5 Data processing

140 The measured raw time series data from the MOS were smoothed using simple exponential smoothing according to Eq. (2):

$$s_t = \alpha x_t + (1-\alpha)s_{t-1} \text{ for } t > 0 \quad (2)$$

145 where s_t is the smoothed CH_4 concentration value (ppm), α is the smoothing factor and s_{t-1} is the previous smoothed CH_4 concentration value (ppm). At time zero ($t=0$), the s_t is equal to the first unsmoothed raw CH_4 value of the MOS. The optimum value for α was determined using Microsoft Excel solver, by minimizing the total average root mean square error (RMSE) between the raw data from the MOS and the simultaneous concentration measurement of the CRDS. Results show an optimal value of 0.042, which for the sake of simplicity was rounded to 0.05, and subsequently used for both the CRDS and MOS data series (Fig. 7).



150 3. Results and Discussion

3.1 Laboratory calibration test of the MOS

Fig. 3 shows the relationship between the resistance ratio (R_S/R_O) for the step test at three humidity levels, where R_O is calculated for each humidity levels based on the average voltage output of the sensor in the time steps where it was exposed to the CH_4 -free synthetic air. It is observed that a near identical response function can be obtained across the three different water vapor concentrations in the air, as long as the water concentration of the zero gas is the same as in the span gas. Based on existing knowledge of the expected air temperature variations at the in situ sampling point at the GrIS (Christiansen and Jørgensen, 2018), the humidity calibration was only carried out at a single temperature in this study. However, variations in the ambient air temperature is also expected to have a linear scaling effect for the type MOS system tested in this study (van den Bossche et al., 2017).

3.2 Field-calibration of the metal oxide sensor

The measured R_S/R_{O^*} ratios per time step over the field calibration period were converted into absolute CH_4 concentrations using the regression statistics of the applied power model (Fig. 6). While the same regression model equations are applied in both the laboratory calibration and field calibration, significant deviation in the model parameters are observed between the laboratory calibration as a group and the field calibration. The reason for this difference is unknown, but a possible explanation could be the potential difference in input heater voltage for the MOS sensor (i.e. pin 1 and 4 in Fig. 1) which has been reported to linearly scale the CH_4 concentration measurements study (van den Bossche et al., 2017). In the laboratory test, the heater circuit of the MOS was supplied by the 5 volt regulated output from the CR1000 datalogger, whereas the heater circuit was supplied from the Arduino Uno's 5 volt regulated output. Future test should aim to investigate if the differences between the results from the laboratory and field calibration can be minimized by using the same type of datalogger and identical power supply (fx. Rechargeable lithium ion battery pack) both in the laboratory and in the field. Results from this type of test could reveal if field calibration for each individual MOS system is needed, or if batch calibrations of several identical MOS-system can be performed in the laboratory without the need for time-consuming field calibration.

3.3 Time-series plot of CH_4 concentration from reference CRDS and MOS

Due to the dynamic environment at the margin of the GrIS, the physical configuration of the sampling point will vary both over the melt-season as well as on an inter-annual basis. In our previous study, high frequency variations in CH_4 concentrations in the subglacial air were observed in a downward draping curve style where a high concentration plateau was interrupted by



180 rapid decreases in CH₄ concentration (Christiansen and Jørgensen, 2018). This pattern was interpreted to be an effect of micro-
turbulent and wind driven dilution of the sample gas in the ice cave by atmospheric air with a CH₄ concentration of
approximately 1.9 ppm. In the current study, exponential smoothing of the raw values is used to compensate for the potential
effects of physical disturbance of the sample gas caused by wind driven turbulent mixing of atmospheric background air at the
subglacial sample point. Also, temporal smoothing can compensate for some of the sensor specific variation in response time
185 improving the pairwise measurement comparability between the CRDS and the MOS. According to the manufacturer, the
CRDS is specified to have a response time of less than 1 hz, while the response time of the MOS is expected to be slower. The
T₉₀ response time for a similar SnO₂-based CH₄ sensor separated with a thin silicone membrane has been reported to be between
1-30 minutes (Boulart et al., 2010), for which the shorter time range is comparable to what is observed in the laboratory
calibration of this study (Fig. 4).

190

The time series plot of the raw and exponentially smoothed CH₄ data from the CRDS (CRDS_{smooth}) is shown together with the
pairwise error between the raw data and the smoothed data (Fig. 7a). Similarly, the time series plot of the raw and exponentially
smoothed CH₄ data from the MOS (MOS_{smooth}) is shown together with the pairwise error between the raw data and the
smoothed data (Fig. 7b). It is generally observed that over the first 4 days of the calibration test, very low differences are
195 observed between the raw data CH₄ concentration and the smoothed CH₄ concentrations for both CRDS_{smooth} and MOS_{smooth},
with absolute errors below 5 ppm (Fig. 7a & 7b). At the end of the field calibrations, higher errors are observed following the
larger spread in CH₄ concentration measurements of both the CRDS and the MOS. CRDS analyzers across different brands
and manufacturers generally perform very consistently and have a highly linear measurement response across the effective
concentration range without any tendencies for increasing analytical error with increasing gas concentrations (Brannon et al.,
200 2016). Fluctuations in CH₄ concentrations in the subglacial air were also observed in (Christiansen and Jørgensen, 2018) using
a CRDS from another manufacturer (G4301 GasScouter, Picarro Inc.). These variations were attributed to the dynamic and
micro-turbulent environment in the subglacial cavity where the gas concentrations were measured and are likely produced by
both air movement generated by the shear stress of the running meltwater as well as turbulent intrusion of atmospheric air
generated by shifting winds speeds at the measurement location at the ice margin.

205

According to the field notes for the current study, a shift in overall wind regime took place during the 25th of June 2018, where
the weather shifted from calm and sunny conditions to more windy conditions dominated by strong catabatic easterly winds
coming off the GrIS. A best estimate of the overall time period where more windy conditions occurred during the field
calibration period is indicated with grey background in Fig. 7. Unfortunately, no direct measurements of wind movement were
210 made during the fieldwork period at the location. Measurements of air temperature at the sample inlet point in the subglacial
cavity (Fig. 7c) shows that an initial period with diurnal temperature variations of approximately 0.1 to 0.2 °C was followed
by a period with more fluctuating temperature variations of up to + 0.6 °C. The period with higher variability corresponds to
the period where higher winds speeds predominate and the deviations between the raw and smoothed CH₄ are the greatest.



215 The higher variability in air temperature measurements during the more windy weather is interpreted as being a product of
more turbulent wind conditions right at the margin of the GrIS and opening to the subglacial cavity by which higher amounts
of warmer atmospheric air with an approximate CH₄ concentration of approximately 1.9 ppm is introduced into the subglacial
cavity. The introduction of these atmospheric air masses results in both short-term temperature increases as well as dilution of
the subglacial CH₄ concentration in the cavity producing the more variable CH₄ concentration patterns observed in both the
CRDS and MOS raw data. In the absence of direct measurements of wind speed and micro-turbulence at the margin of the ice,
220 rapid variations in air temperature at the sample inlet point with an amplitude greater than the 0.2 °C appear as a reasonable
indicator or proxy for micro-turbulent dilution and physical disturbance of the source signal, which can effectively be filtered
out by the application of exponential smoothing.

The relative error between each MOS_{smooth} and CRDS_{smooth} measurement pair can be expressed as the percentage that the
225 difference constitutes compared to the reference CRDS concentration (i.e. $\text{MOS}_{\text{smooth}} - \text{CRDS}_{\text{smooth}} / \text{CRDS}_{\text{smooth}} \times 100$). It is
seen that the pairwise relative error between the MOS_{smooth} and CRDS_{smooth} shows similar non-systematic variations in both
the calm weather and windy time period with relative errors typically below $\pm 10\%$ (Fig. 7d). This result show both that the
accuracy of the CH₄ concentration measured by the MOS are in close agreement with the reference CRDS and that the
exponential smoothing effectively compensates for short term physical disturbances at the measurement point. The result also
230 indicate that no systematic drift or over/underestimation is apparent when comparing the MOS_{smooth} to the CRDS_{smooth} over the
100 h field calibration period (Fig. 7b). When considering the magnitude of the absolute errors between the raw and smoothed
CH₄ concentration for both the CRDS and the MOS, together with the temporal pattern in the development of the relative
error, it shows that the high frequency concentration fluctuations measured with the MOS are most likely the product of
physical disturbances at the measurement point (primary sampling error), and not by an analytical error introduced by the
235 MOS itself (secondary sampling error).

As supplement to the pairwise error comparison, average time-series performance statistics for the difference between the
MOS_{smooth} and CRDS_{smooth} time series can be calculated for both the full field calibration period, as well for the non-turbulent
time period with limited observed physical disturbance at the sampling point (Table 1). Mean bias errors for both the non-
240 turbulent and full time series are approximately ± 0.01 ppm CH₄ with standards deviations of ± 1.3 to 1.7 ppm CH₄ respectively.

3.4 Post-correction and cross-interference evaluation

One of the main obstacles previously reported concerning the use of MOS's for monitoring of gases in ambient air is the
possible effect of variations in air temperature and humidity in the sampling environment (Masson et al., 2015; Sohn et al.,
245 2008). One approach to compensate for this potential measurement error is to post-correct for variations in temperature and
humidity, based on either generic temperature and humidity dependency curves supplied by the sensor company (Eugster and



Kling, 2012) or by performing sensor calibrations under controlled levels of temperature and humidity in the laboratory (van den Bossche et al., 2017).

250 Measurements from the air-filled cavity under the GrIS document a very stable sampling environment with a relative humidity throughout the sampling period of close to 100 % RH (data not shown) and only minor air temperature variations between approximately 0.05 °C during the night and 0.25 °C during mid-day (Fig. 7d). Because of these stable and well-buffered environmental conditions, no post-corrections due to variations in temperature and relative humidity are evaluated to be necessary for this particular sampling environment.

255 Observed variations in maximum air temperature in the subglacial cavity correspond to field observation of the time of the day when maximum meltwater discharge occurs. We assume that the observed temperature pattern reflects the impact of thermal heat diffusion from this running meltwater to the air immediately above, but would need direct measurements of the daily variations in meltwater temperature to verify this assumption.

260 The emitted CH₄ may originate from both thermogenic and/or biogenic sources below the GrIS. If the primary source of CH₄ is thermogenic, the emission may also be accompanied by more complex hydrocarbons, including ethane (C₂H₆), while this will not be the case if the source is biogenic (Hopkins et al., 2016). Since the MOS used in the study is non-selective to CH₄ due to its basic principle of operation (Eugster and Kling, 2012; Wang et al., 2010), the presence of other hydrocarbons such as ethanol (C₂H₆O), isobutene (C₄H₁₀) and potentially also other low molecular weight alkanes could potentially cause cross-interference with the CH₄ measurement. It follows, that if the source of the CH₄ that is emitted for the subglacial domain originates in thermogenic natural gas reservoirs under the GrIS, the other non CH₄-hydrocarbons could potentially affect the measurements performed by the MOS, while passing non-detected by the CRDS. However, since the magnitudes and temporal patterns in CH₄ concentrations are similar in both the CRDS and MOS it is assumed that the gases emitted from the subglacial domain are primarily CH₄ and CO₂ with very limited potential for cross-interference from other hydrocarbon gases. Also, isotopic analysis of the emitted CH₄ and CO₂ in (Lamarche-Gagnon et al., 2018) as well as unpublished data from this study, have shown that the emitted CH₄ is dominantly of microbial origin and has isotopic similarity to CH₄ produced by anaerobic decomposition of organic carbon in wetlands. It is therefore assumed that there is no need for any post correction of the CH₄ concentrations measured by the MOS in this type of environment due to lack of cross-interference from other hydrocarbon gases.

275

3.5 Autonomous CH₄ monitoring using MOS system

The combined time period in which CH₄ concentrations were measured can be divided into three separate periods depending on the analytical devices used, namely period 1 corresponding to the field calibration period where both the CRDS and MOS



280 were in operation (approximately 100 h), period 2 where only the CRDS was in operation (approximately 24 h) and period 3
where only the MOS was in operation (Fig. 8). Continuous CH₄ data from period 3 exist for the period 27th June to 15th July
2018. When comparing the combined CH₄ concentration curves from all three periods it is observed that the CRDS_{smooth} and
MOS_{smooth} follow each other as described above (Fig. 7). CRDS_{smooth} data for period 2 fills the data gap between the MOS
measurement of period 1 and 3, where the MOS_{smooth} concentration data departs very close to the concentration level where
285 the CRDS_{smooth} measurements end. Due to the nature of the study design and difficult access to the remote field site at the GrIS,
the accuracy and precision of the MOS_{smooth} cannot be evaluated for the period 3 where only the MOS system was operating.
However, the pattern in which subglacial CH₄ concentrations varied and the estimated minimum and maximum values appear
similar to the values of the calibration period. When comparing the complete time period of this study to e.g. Eugster and Kling
(2012), no significant sensor drift is expected over the monitoring time period. Additional and extended field work at the GrIS
290 with repeated calibration at the end of the field deployment period is needed to quantify the potential sensor drift, as well as
stability range over longer time scales. Nonetheless, the observed performance of the MOS during the calibration period with
ppm-level accuracies and subsequent trouble-free operation running as an autonomous unit shows that this type of low-cost
and low-power CH₄ sensing system holds a great potential for the further development and refinement of a greater sensor
network at representative meltwater outlets at the Greenland ice Sheet. The major scientific scope of this performance test is
295 that we can demonstrate a realistic low-cost technical solution for closing one of the most critical knowledge gaps in the Arctic
carbon budget, namely the climatic impact of CH₄ emissions to the atmosphere under both current and future warmer climatic
conditions.

The next steps and lessons learned from this study deals with the further development of the low-power system for actual CH₄
emission measurements, which involves measurements of air volume and meltwater discharge as well as continuous
300 measurements of the dissolved CH₄ in the meltwater, similar to (Lamarche-Gagnon et al., 2018). Also, optimizing the
positioning of gas sensing equipment at the measurement point should be done to reduce the potential physical disturbances
due to micro-turbulence and intrusion of atmospheric air in the subglacial cavity. Furthermore, an improved adjustment scheme
should be developed to account for the dynamic melt back of the ice margin over the melt season, which requires either manual
305 or automated sample point relocation to keep the sampling point at an optimal physical location. Finally, more work is needed
to test what modification to the systems are needed to establish a universal calibration curve in the laboratory, so that the need
for field calibration with the reference CRDS can be eliminated.



4. Conclusions

310 Recent discoveries at the Greenland Ice Sheet (GrIS) have revealed a so far overlooked source of CH₄ from the subglacial
domain under the ice to the atmosphere. Development of low-power CH₄ monitoring systems based on low cost metal oxide
sensors (MOS) could enable the development of a sensor network at representative meltwater outlets at the GrIS which
significantly could enhance the fundamental understanding of the phenomena's climatic importance. In the current study, the
performance of a metal oxide sensor sensitive to CH₄ was tested in an air-filled cavity at the edge of the Greenland Ice Sheet
315 over an initial field calibration period of approximately 100 h using both a reference gas analyzer based on cavity ring-down
spectroscopy (CRDS) and a low-cost metal oxide sensor (MOS) followed by a period of autonomous CH₄ concentration
monitoring using only the MOS system. Parallel measurements using a common inlet show good agreement between the MOS
and the CRDS over time under the stable environmental conditions under the ice. Exponential smoothing of the raw data from
both the CRDS and MOS effectively remove high frequency concentration variations induced by physical disturbance of the
320 air in the subglacial cavity under more turbulent wind conditions at the margin of the ice sheet. Based on concentration values
of the smoothed CRDS and MOS data, the pairwise measurement errors were generally below ± 5 ppm CH₄ between the MOS
and the CRDS reference value. Pairwise relative errors were generally below ± 10 % between the MOS and the CRDS reference
value. The mean bias error for the entire field calibration period was -0.05 ppm CH₄ with a standard deviation of ± 1.69 ppm
CH₄. If only data for the non-turbulent time period was evaluated, the mean bias error was 0.09 ppm CH₄ with a standard
325 deviation of ± 1.35 ppm CH₄. Due to the very clean and stable sampling environment in the air-filled cavity under the
Greenland Ice Sheet, no post-corrections for variations in air temperature, humidity or cross interference from other
hydrocarbon gases were needed for the MOS measurements. Combined with measurement of airflow and meltwater discharge,
the measurement of CH₄ concentrations can be used for determination of the mass flux of CH₄ to the atmosphere. The study
demonstrates a clear potential for expanded monitoring of spatial and temporal variation in CH₄ emissions from the subglacial
330 domain of the Greenland Ice Sheet using low-cost and low-power MOS.

5. Author contribution

CJJ and JRC designed and carried out the field experiments. CJJ, JMO and KFU planned and carried out the laboratory
calibrations. CJJ and JRC prepared the manuscript with contributions from all co-authors.

6. Acknowledgements

335 This work was supported by a research grant from the “Brødrene Hartsmanns Fond” for the project “Udledning af metan til
atmosfæren fra gletchere” and performed as part of the “Arctic Research Centre” and “iClimate” research frameworks at
Aarhus University. Laboratory test of MOS sensors was performed by FORCE Technology through support from the Danish
Agency for Innovation as part of the project “Den Danske Renluftsektor”.



340 7. References

- van den Bossche, M., Rose, N. T. and De Wekker, S. F. J.: Potential of a low-cost gas sensor for atmospheric methane monitoring, *Sensors Actuators, B Chem.*, 238(2), 501–509, doi:10.1016/j.snb.2016.07.092, 2017.
- Boulart, C., Connelly, D. P. and Mowlem, M. C.: Sensors and technologies for in situ dissolved methane measurements and
345 their evaluation using Technology Readiness Levels, *TrAC - Trends Anal. Chem.*, 29(2), 186–195, doi:10.1016/j.trac.2009.12.001, 2010.
- Brannon, E. Q., Moseman-valtierra, S. M., Rella, C. W., Martin, R. M., Chen, X. and Tang, J.: Evaluation of laser-based spectrometers for greenhouse gas flux measurements in coastal marshes, *Limnol. Ocean. METHODS*, 14, 466–476, doi:10.1002/lom3.10105, 2016.
- 350 Callaghan, T. V., Johansson, M., Key, J., Prowse, T., Ananicheva, M. and Klepikov, A.: Feedbacks and Interactions: From the Arctic Cryosphere to the Climate System, *Ambio*, 40(S1), 75–86, doi:10.1007/s13280-011-0215-8, 2011.
- Christiansen, J. R. and Jørgensen, C. J.: First observation of direct methane emission to the atmosphere from the subglacial domain of the Greenland Ice Sheet, *Sci. Rep.*, 8(1), 16623, doi:10.1038/s41598-018-35054-7, 2018.
- Emmerton, C. A., St. Louis, V. L., Lehnerr, I., Humphreys, E. R., Rydz, E. and Kosolofski, H. R.: The net exchange of
355 methane with high Arctic landscapes during the summer growing season, *Biogeosciences*, 11(12), 3095–3106, doi:10.5194/bg-11-3095-2014, 2014.
- Eugster, W. and Kling, G. W.: Performance of a low-cost methane sensor for ambient concentration measurements in preliminary studies, *Atmos. Meas. Tech.*, 5(8), 1925–1934, doi:10.5194/amt-5-1925-2012, 2012.
- Hopkins, F. M., Kort, E. A., Bush, S. E., Ehleringer, J. R., Lai, C. T., Blake, D. R. and Randerson, J. T.: Spatial patterns and
360 source attribution of urban methane in the Los Angeles Basin, *J. Geophys. Res.*, 121(5), 2490–2507, doi:10.1002/2015JD024429, 2016.
- Juncher Jørgensen, C., Lund Johansen, K. M., Westergaard-Nielsen, A. and Elberling, B.: Net regional methane sink in High Arctic soils of northeast Greenland, *Nat. Geosci.*, 8(1), 20–23, doi:10.1038/ngeo2305, 2015.
- Kumar, R., Imam, S. A. and Khan, M. R.: “A Critical Review of Taguchi Gas Sensor for the Detection of VOC’s,” *MASAUM*
365 *J. Rev. Surv.*, Vol 1(No. 2), 177–183, doi:10.1007/s11926-016-0595-7, 2009.
- Lamarche-Gagnon, G., Wadham, J. L., Lollar, B. S., Arndt, S., Fietzek, P., Beaton, A. D., Tedstone, A. J., Telling, J., Bagshaw, E. A., Hawkings, J. R., Kohler, T. J., Zarsky, J. D., Mowlem, M. C., Anesio, A. and Stibal, M.: Greenland melt drives continuous export of methane from its bed, *Nature*, In press, doi:10.1038/s41586-018-0800-0, 2018.
- Masson, N., Piedrahita, R. and Hannigan, M.: Approach for quantification of metal oxide type semiconductor gas sensors used
370 for ambient air quality monitoring, *Sensors Actuators B Chem.*, 208, 339–345, doi:10.1016/J.SNB.2014.11.032, 2015.



- Penza, M., Suriano, D., Cassano, G., Pfister, V., Amodio, M., Trizio, L., Brattoli, M. and De Gennaro, G.: A case-study of micro-sensors for landfill air-pollution monitoring applications, *Urban Clim.*, 14, 351–369, doi:10.1016/j.uclim.2014.09.002, 2015.
- Peterson, P., Aujla, A., Grant, K., Brundle, A., Thompson, M., Vande Hey, J. and Leigh, R.: Practical Use of Metal Oxide Semiconductor Gas Sensors for Measuring Nitrogen Dioxide and Ozone in Urban Environments, *Sensors*, 17(7), 1653, doi:10.3390/s17071653, 2017.
- Pirk, N., Mastepanov, M., López-Blanco, E., Christensen, L. H., Christiansen, H. H., Hansen, B. U., Lund, M., Parmentier, F.-J. W., Skov, K. and Christensen, T. R.: Toward a statistical description of methane emissions from arctic wetlands, *Ambio*, 46(S1), 70–80, doi:10.1007/s13280-016-0893-3, 2017.
- 380 Saunois, M., Bousquet, P., Poulter, B., Peregón, A., Ciais, P., Canadell, J. G., Dlugokencky, E. J., Etiope, G., Bastviken, D., Houweling, S., Janssens-Maenhout, G., Tubiello, F. N., Castaldi, S., Jackson, R. B., Alexe, M., Arora, V. K., Beerling, D. J., Bergamaschi, P., Blake, D. R., Brailsford, G., Brovkin, V., Bruhwiler, L., Crevoisier, C., Crill, P., Covey, K., Curry, C., Frankenberg, C., Gedney, N., Höglund-Isaksson, L., Ishizawa, M., Ito, A., Joos, F., Kim, H.-S., Kleinen, T., Krummel, P., Lamarque, J.-F., Langenfelds, R., Locatelli, R., Machida, T., Maksyutov, S., McDonald, K. C., Marshall, J., Melton, J. R.,
- 385 Morino, I., Naik, V., O’Doherty, S., Parmentier, F.-J. W., Patra, P. K., Peng, C., Peng, S., Peters, G. P., Pison, I., Prigent, C., Prinn, R., Ramonet, M., Riley, W. J., Saito, M., Santini, M., Schroeder, R., Simpson, I. J., Spahni, R., Steele, P., Takizawa, A., Thornton, B. F., Tian, H., Tohjima, Y., Viovy, N., Voulgarakis, A., Van Weele, M., Van Der Werf, G. R., Weiss, R., Wiedinmyer, C., Wilton, D. J., Wiltshire, A., Worthy, D., Wunch, D., Xu, X., Yoshida, Y., Zhang, B., Zhang, Z. and Zhu, Q.: The global methane budget 2000–2012, *Earth Syst. Sci. Data*, 8, 697–751, doi:10.5194/essd-8-697-2016, 2016.
- 390 Sohn, J. H., Atzeni, M., Zeller, L. and Pioggia, G.: Characterisation of humidity dependence of a metal oxide semiconductor sensor array using partial least squares, *Sensors Actuators B Chem.*, 131(1), 230–235, doi:10.1016/J.SNB.2007.11.009, 2008.
- Wadham, J. L., Hawkings, J. R., Tarasov, L., Gregoire, L. J. and Spencer, R. G. M.: Ice sheets matter for the global carbon cycle, *Nat. Commun.*, doi:10.1038/s41467-019-11394-4, 2019.
- Wang, C., Yin, L., Zhang, L., Xiang, D. and Gao, R.: Metal oxide gas sensors: sensitivity and influencing factors., *Sensors (Basel)*, 10(3), 2088–106, doi:10.3390/s100302088, 2010.
- Zona, D., Gioli, B., Commane, R., Lindaas, J., Wofsy, S. C., Miller, C. E., Dinardo, S. J., Dengel, S., Sweeney, C., Karion, A., Chang, R. Y.-W., Henderson, J. M., Murphy, P. C., Goodrich, J. P., Moreaux, V., Liljedahl, A., Watts, J. D., Kimball, J. S., Lipson, D. A. and Oechel, W. C.: Cold season emissions dominate the Arctic tundra methane budget, *Proc. Natl. Acad. Sci.*, 113(1), 40–45, doi:10.1073/pnas.1516017113, 2016.



Figure captions

405

Figure 1: Overview of the sampling location at Isunnguata Sermia Glacier at the western margin of the Greenland Ice sheet during June 2018. (a) Location of sampling region the island of Greenland, (b) regional location of the outlet glacier, (c) location of the meltwater outlet at Isunnguata Sermia and (d) local sample location with investigated subglacial cavity marked with red circle. Source of (a), (b) and (c): Google Earth, earth.google.com/web/.

410

Figure 2: (a) Close-up of air-filled cavity below the Greenland Ice Sheet next to the lateral meltwater outlet. The aluminum pole extends approximately 5 meters into the cavity and holds the inlet tube and the temperature and humidity smart sensor. (b) Conceptual diagram of the MOS system placement in an enclosure constantly flushed by the outflow from the CRDS analyzer (c) Close-up of the board mounted MOS and temperature/humidity micro sensor. The MOS system consisted of 1) a microcontroller, 2) Datalogger shield holding metal oxide CH₄ sensor and 3) an additional temperature/relative humidity micro sensor.

415

420

Figure 3: Simplified schematic of the metal oxide sensor (MOS) system consisting of a TGS2611-E00 with pin 3 and 4 connected to the 5-volt output of the Arduino Uno, pin 1 connected to ground and pin 2 connected to the analogue input of the Arduino Uno and a 10kOhm load resistor, which also connects to ground.

425

Figure 4: Outlet voltages of the MOS during laboratory step calibration at stabilized levels of relative humidity ($37 \pm 2\%$, $55 \pm 3\%$ and $76 \pm 3\%$) in both the zero and span gas at alternating concentration of CH₄ in the calibration gas between 10 and 100 ppm CH₄. Each time step lasted 10 min and sequences with grey shadings show time periods where the sensor was exposed to CH₄ free zero gas.

430

Figure 5: Resistance ratio of MOS as three levels of relative humidity at CH₄ concentration levels between 10 to 100 ppm CH₄ in humidified synthetic air.

435

Figure 6: Regression plot of calculated MOS resistance ratio R_s/R_{O^*} vs. the reference in situ CH₄ concentrations from the CRDS.

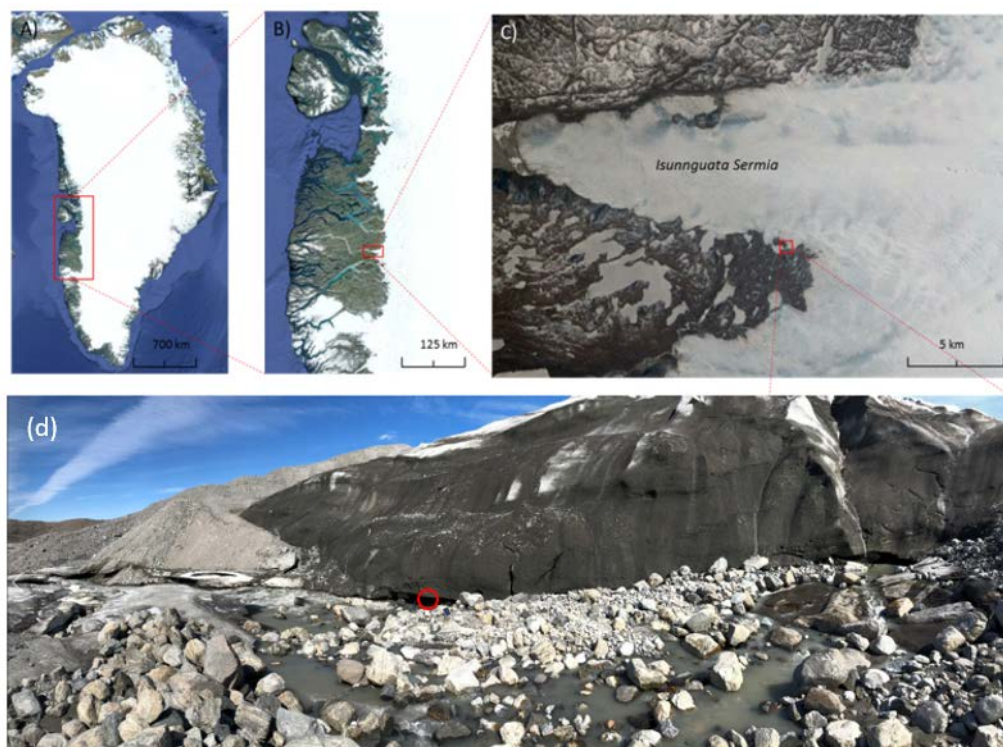
440

Figure 7: (a) Grey dots show raw CH₄ concentration from CRDS. Black line show CRDS CH₄ concentration values following exponential smoothing. Black bars show absolute error between raw and smoothed values. (b) Grey dots show calculated raw CH₄ concentration from MOS. Black line show MOS CH₄ concentration values following exponential smoothing. Black bars show absolute error between raw and smoothed values. (c) Black dots show temperature of air in subglacial cavity. (d) Black bars show the relative error in percentage between the MOS_{smooth} and $CRDS_{smooth}$ divided by the $CRDS_{smooth}$ concentration. Grey background shading indicates period with higher observed turbulence at the margin of the GrIS.

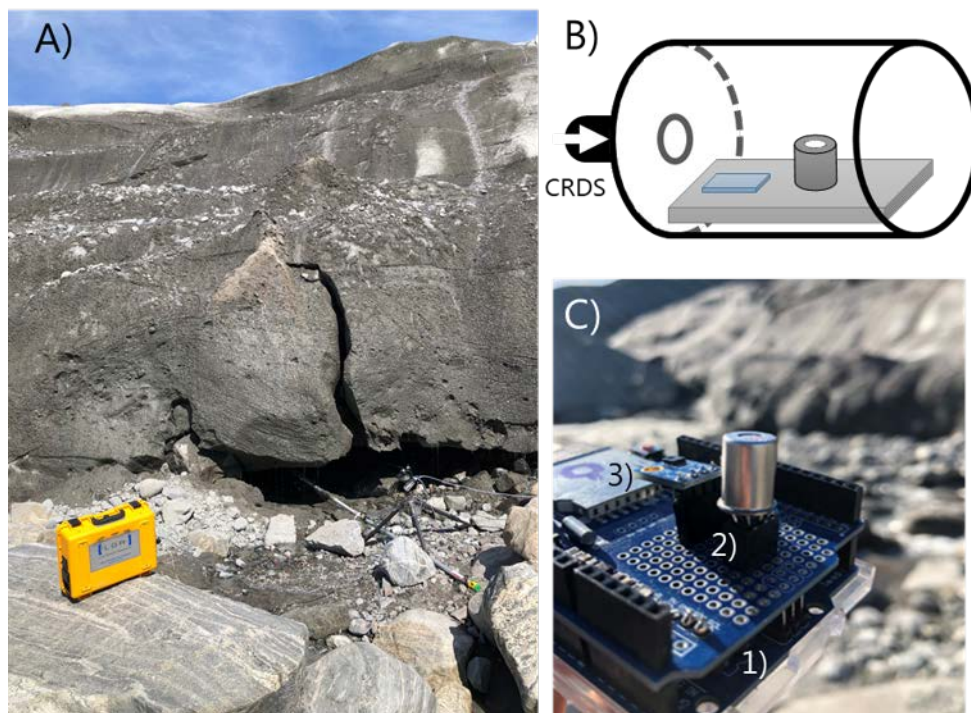
445

Figure 8: Smoothed time series measurements of CH₄ at the Greenland Ice Sheet using both the cavity ring-down spectroscopy (CRDS) reference monitor and the metal oxide sensor (MOS).

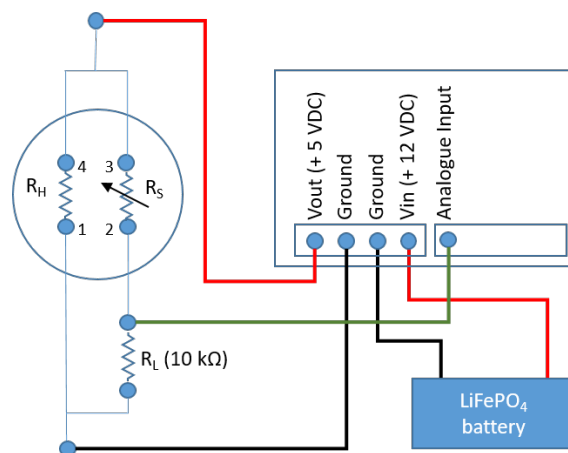
Table 1. Statistics for the calculated differences between the smoothed MOS and smoothed CDRS data series in both the non-turbulent time period and full field calibration period. The unit for error and difference values is ppm.



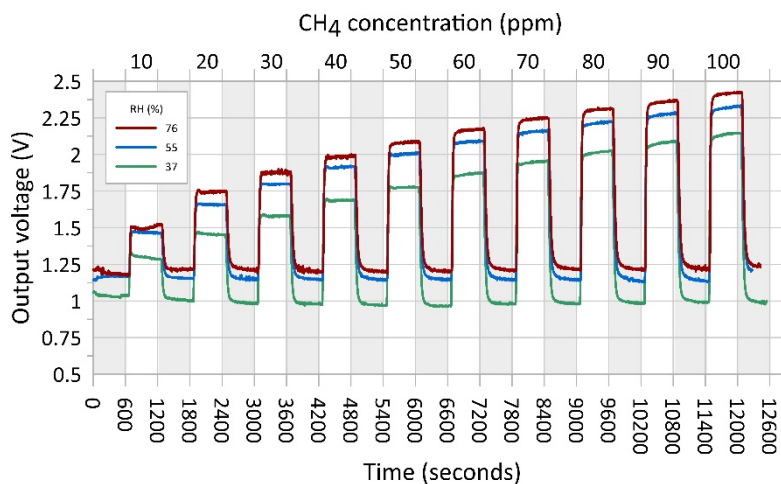
450 Figure 1: Overview of the sampling location at Isunnguata Sermia Glacier at the western margin of the Greenland Ice sheet during June 2018. (a) Location of sampling region the island of Greenland, (b) regional location of the outlet glacier, (c) location of the meltwater outlet at Isunnguata Sermia and (d) local sample location with investigated subglacial cavity marked with red circle. Source of (a), (b) and (c): © Google Earth, earth.google.com/web/.



455 Figure 2: (a) Close-up of air-filled cavity below the Greenland Ice Sheet next to the lateral meltwater outlet. The aluminum
pole extends approximately 5 meters into the cavity and holds the inlet tube and the temperature and humidity smart sensor.
(b) Conceptual diagram of the MOS system placement in an enclosure constantly flushed by the outflow from the CRDS
analyzer (c) Close-up of the board mounted MOS and temperature/humidity micro sensor. The MOS system consisted of 1)
460 a microcontroller, 2) Datalogger shield holding metal oxide CH₄ sensor and 3) an additional temperature/relative humidity
micro sensor.



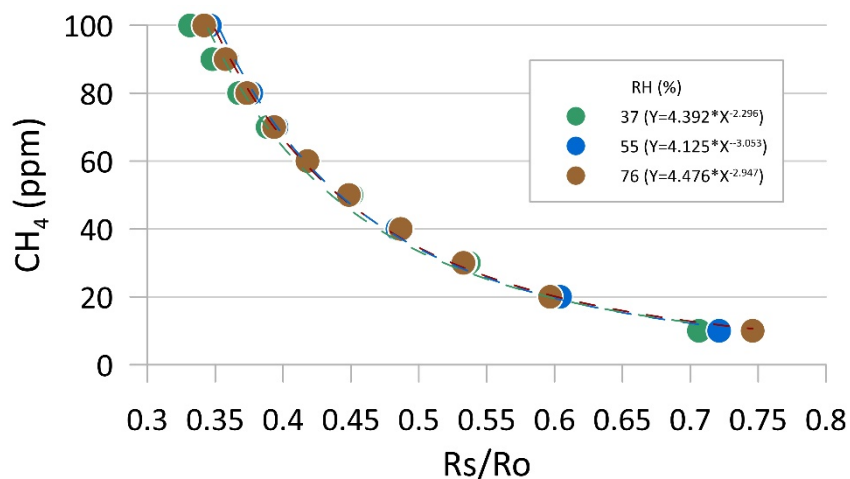
465 Figure 3: Simplified schematic of the metal oxide sensor (MOS) system consisting of a TGS2611-E00 with pin 3 and 4 connected to the 5-volt output of the Arduino Uno, pin 1 connected to ground and pin 2 connected to the analogue input of the Arduino Uno and a 10kOhm load resistor, which also connects to ground.



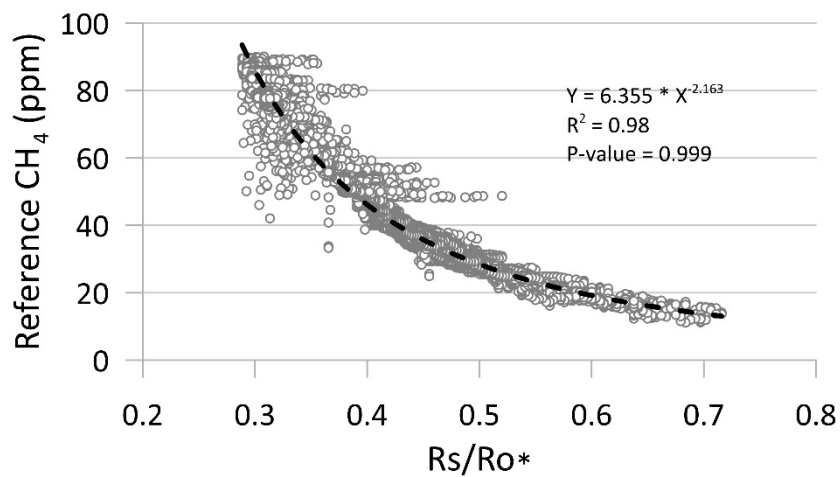
470

Figure 4: Outlet voltages of the MOS during laboratory step calibration at stabilized levels of relative humidity ($37 \pm 2 \%$, $55 \pm 3 \%$ and $76 \pm 3 \%$) in both the zero and span gas at alternating concentration of CH₄ in the calibration gas between 10 and 100 ppm CH₄. Each time step lasted 10 min and sequences with grey shadings show time periods where the sensor was exposed to CH₄ free zero gas.

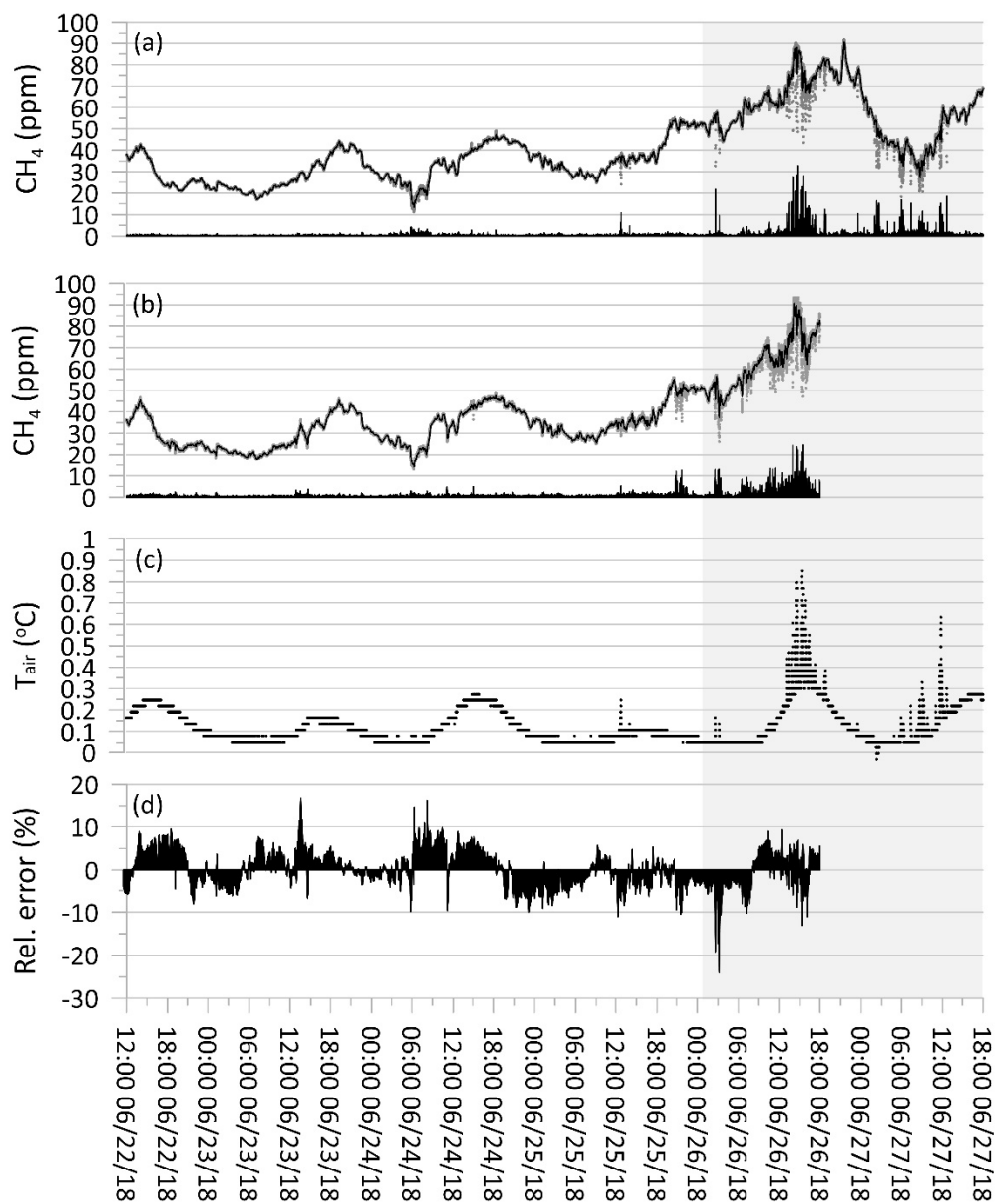
475



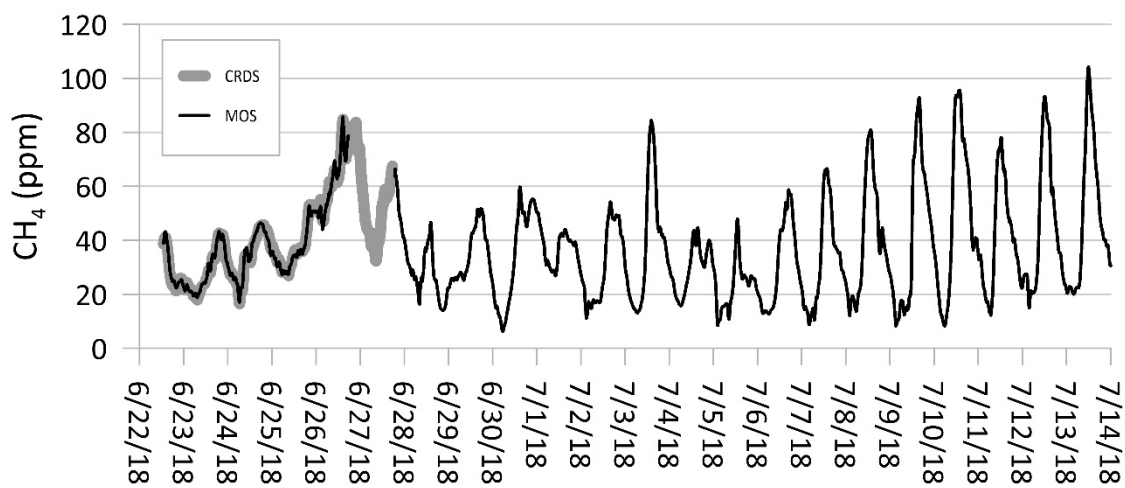
480 Figure 5: Resistance ratio of MOS as three levels of relative humidity at CH_4 concentration levels between 10 to 100 ppm CH_4 in humidified synthetic air.



485 Figure 6: Regression plot of calculated MOS resistance ratio R_s/R_{O^*} vs. the reference in situ CH₄ concentrations from the CRDS.



490 Figure 7: (a) Grey dots show raw CH_4 concentration from CRDS. Black line show CRDS CH_4 concentration values
following exponential smoothing. Black bars show absolute error between raw and smoothed values. (b) Grey dots show
calculated raw CH_4 concentration from MOS. Black line show MOS CH_4 concentration values following exponential
smoothing. Black bars show absolute error between raw and smoothed values. (c) Black dots show temperature of air in
subglacial cavity. (d) Black bars show the relative error in percentage between the $\text{MOS}_{\text{smooth}}$ and $\text{CRDS}_{\text{smooth}}$ divided by the
495 $\text{CRDS}_{\text{smooth}}$ concentration. Grey background shading indicates period with higher observed turbulence at the margin of the
GrIS.



500

Figure 8: Smoothed time series measurements of CH_4 at the Greenland Ice Sheet using both the cavity ring-down spectroscopy (CRDS) reference monitor and the metal oxide sensor (MOS).



505 Tables

Table 1. Statistics for the calculated differences between the smoothed MOS and smoothed CDRS data series in both the non-turbulent time period and full field calibration period. The unit for error and difference values is ppm.

Statistics: $MOS_{smooth} - CRDS_{smooth}$	Non-Turbulent	Full series
Mean bias error	0.09	-0.05
Root mean square error	1.35	1.69
Maximum negative difference	-3.96	-11.83
Maximum positive difference	5.04	5.91
Observations	28501	37140

510